Supporting Information for

3-layer conductive metal-organic nanosheets as electrocatalysts to enable ultralow detection limit of H_2O_2

Mingdao Zhang,[a]* Gang Wang,[b] Baohui Zheng,[c] Longyan Li,[a] Boning Lv,[a] Hui Cao[a]* and Mindong Chen[a]*

[a.] *Department of Chemistry, Jiangsu Key Laboratory of Atmospheric Environment Monitoring and Pollution Control, Collaborative Innovation Center of Atmospheric Environment and Equipment Technology, School of Environmental Science and Engineering, Nanjing University of Information Science & Technology, Nanjing 210044, Jiangsu, PR China. E-mail: matchlessjimmy@163.com; yccaoh@hotmail.com; Chenmd@nuist.edu.cn*

[b.] *Beijing Institute of Information Technology, Beijing 100094, P. R. China.*

[c.] *Institute of Chemical Materials, Chinese Academy of Engineering Physics, Mianyang 621999, Sichuan, P. R. China.*

Additional drawings and figures to support the maintext:

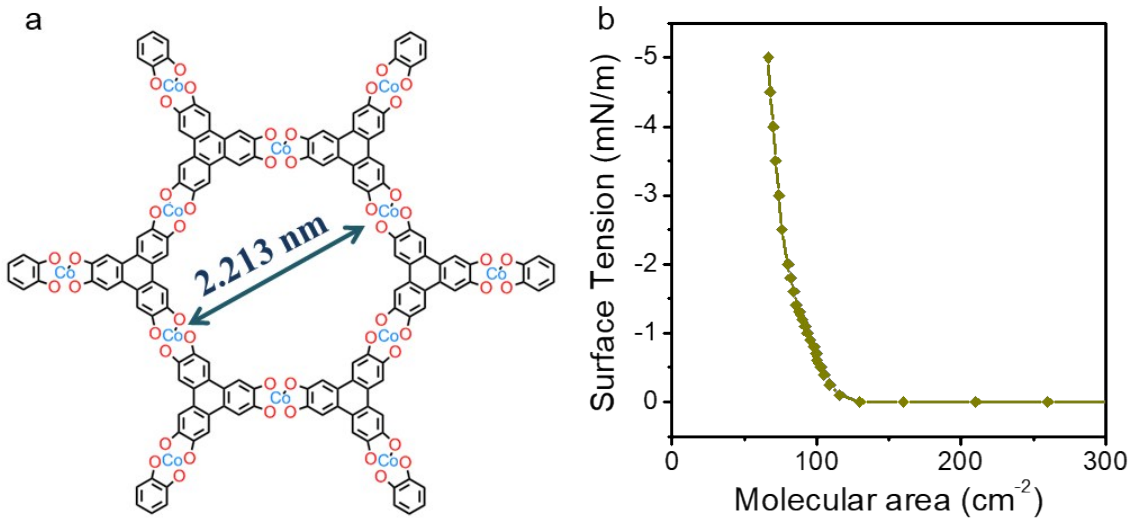

Fig. S1. (a) Hole fragment of the $[Co_3(HHTP)_2]_n$ LB nanosheets. (b) Surface pressure (SP)–mean molecular area (MMA) isotherm of HHTP monomer spread at the air/water interface at room temperature at a compression rate of 2 mm min^{-1}.

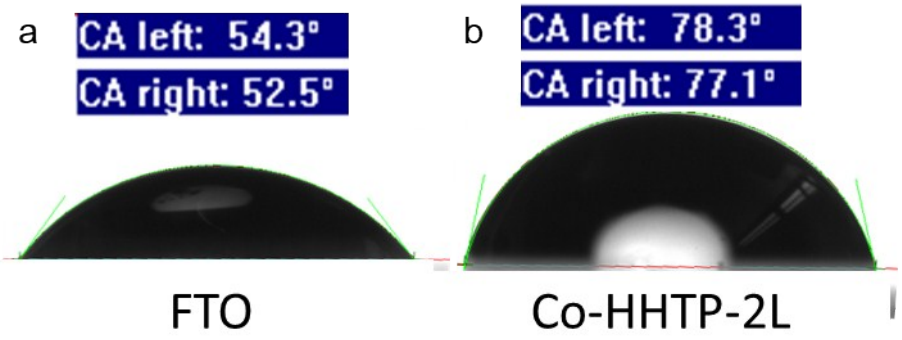

Fig. S2. Water contact angles of (a) FTO glass, (b) double-layer $[Co_3(HHTP)_2]_n$ LB nanosheets.

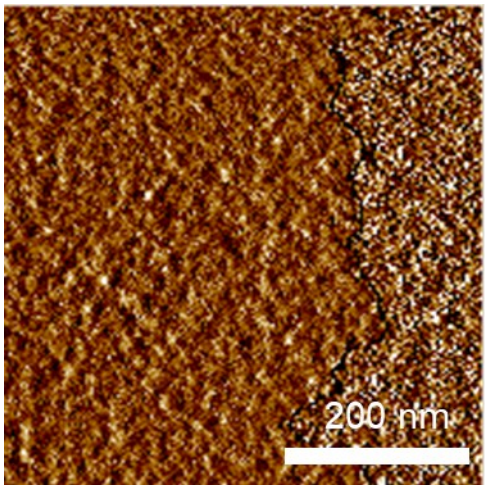

Fig. S3. AFM amplitude image of single-layer $[Co_3(HHTP)_2]_n$ LB nanosheet.

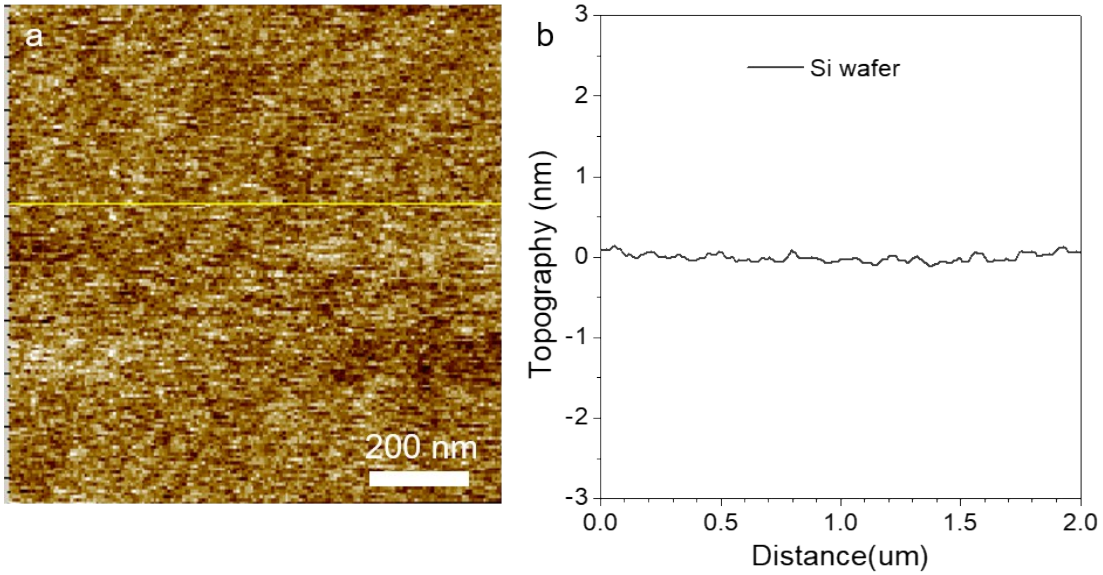

Fig. S4. (a) AFM topography image of single-layer $[Co_3(HHTP)_2]_n$ LB nanosheet. (b) Corresponding line profiles of the nanosheet in S5a.

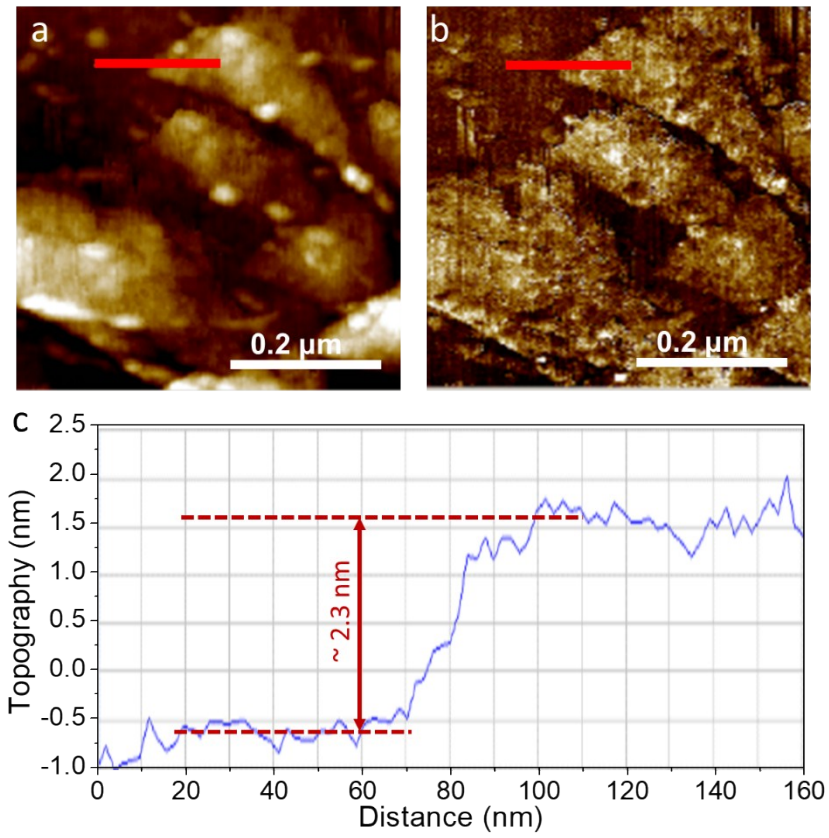

Fig. S5. (a) AFM topography image of 3-layer $[Co_3(HHTP)_2]_n$ LB nanosheets; (b) AFM phase image of 3-layer $[Co_3(HHTP)_2]_n$ LB nanosheets; (c) Corresponding line profiles of the yellow line in Figs. S5a and S5b.

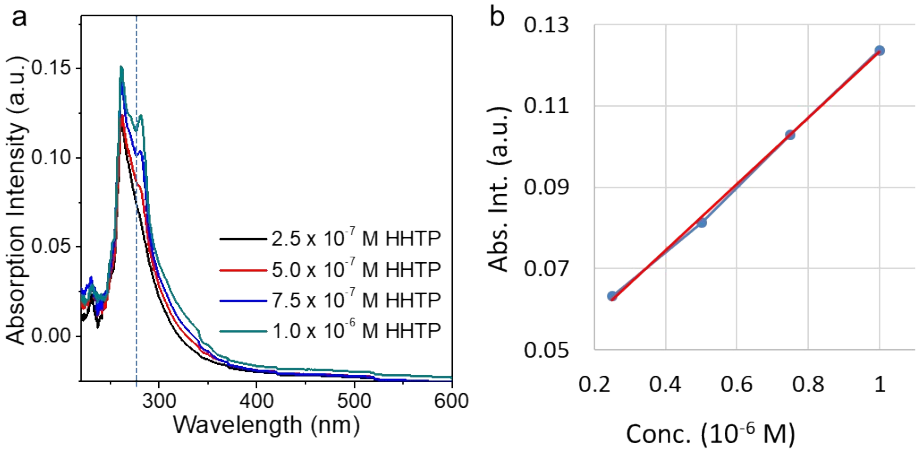

Fig. S6. (a) UV-vis absorption spectra of HHTP solution at different concentration; (b) The linear relationship between the absorbance at 282 nm and the concentration.

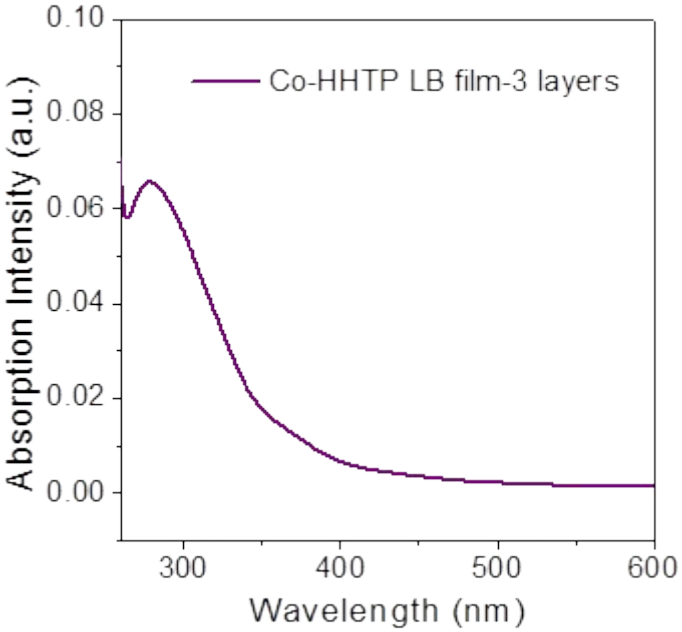

Fig. S7. UV-vis absorption spectra of $[Co_3(HHTP)_2]_n$ LB 3-layer nanosheets

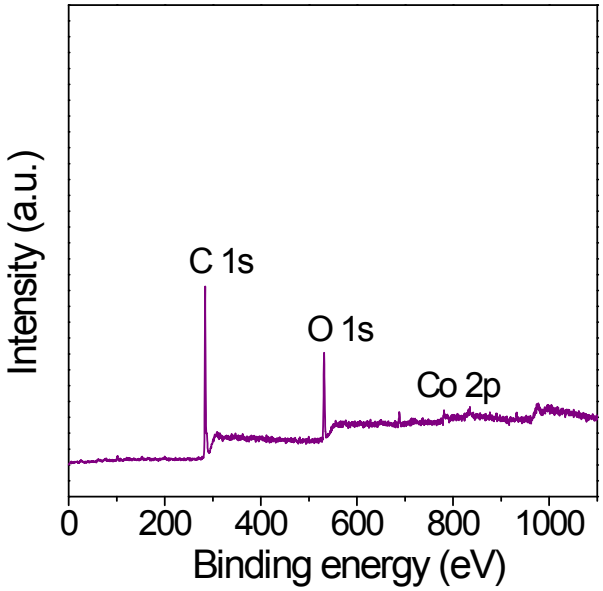

Fig. S8. XPS energy survey spectra of 30-layer $[Co_3(HHTP)_2]_n$ LB nanosheets.

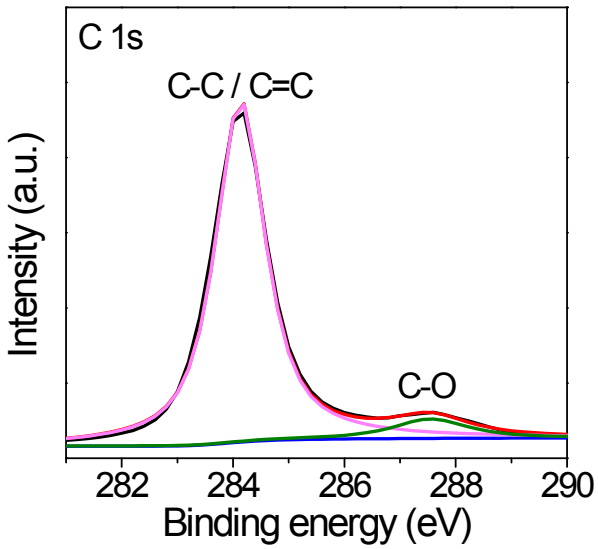

Fig. S9. C 1s spectrum of $[Co_3(HHTP)_2]_n$ LB nanosheets.

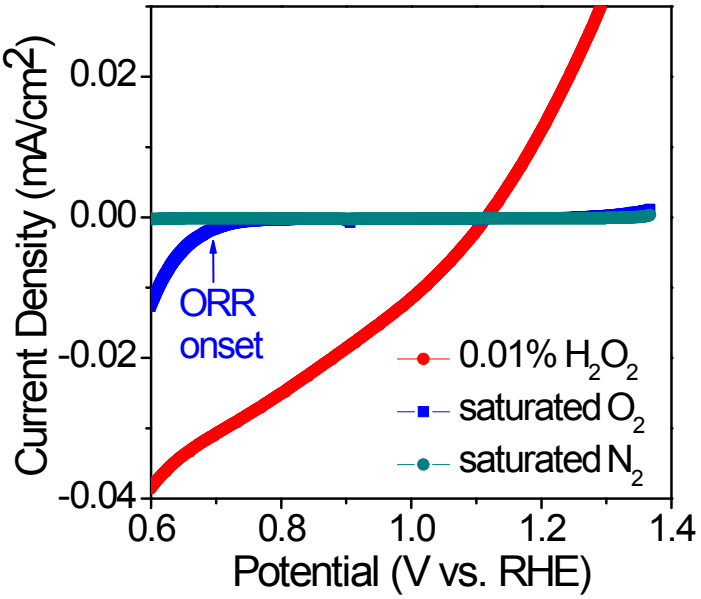

Fig. S10. LSV curves of 1-layer $[Co_3(HHTP)_2]_n$ LB nanosheet in N_2/O_2 saturated and H_2O_2 added 0.1 M KOH.

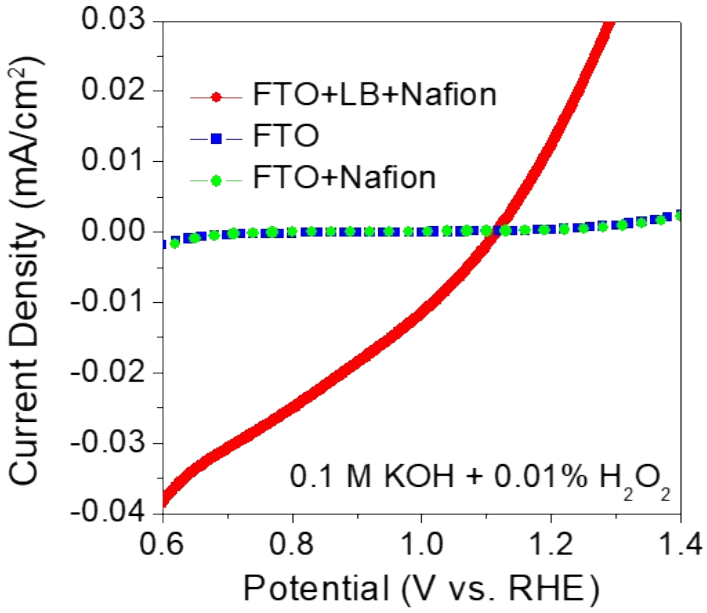

Fig. S11. LSV curves of FTO, FTO+nafion, and FTO+nafion+$[Co_3(HHTP)_2]_n$ LB nanosheets.

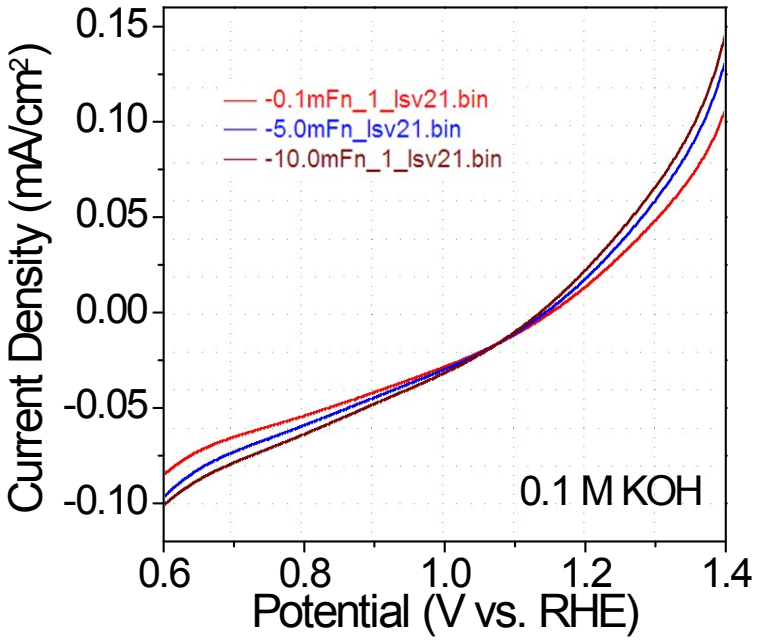

Fig. S12. LSV curves of single-layer $[Co_3(HHTP)_2]_n$ LB nanosheets transferred under different surface tensions.

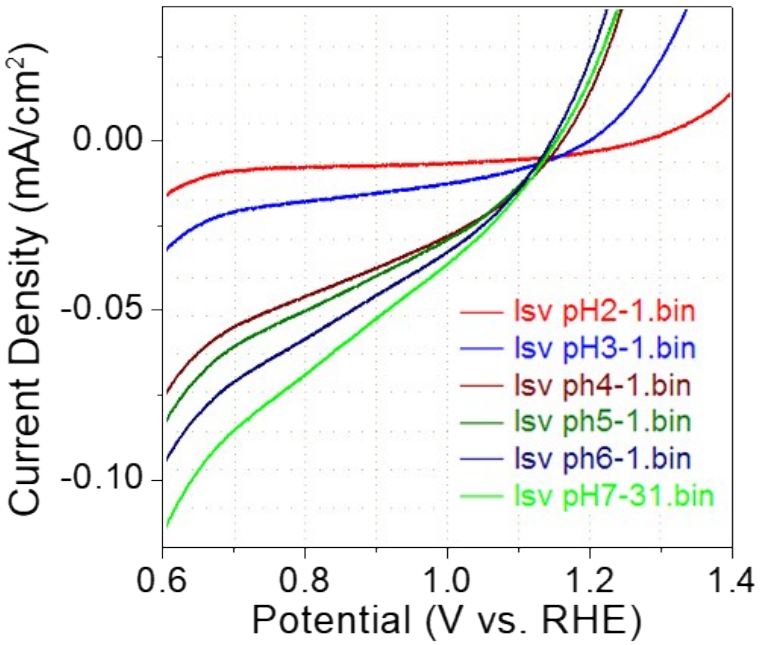

Fig. S13. LSV curves of 3-layer $[Co_3(HHTP)_2]_n$ LB nanosheets tranfered under different pH values.

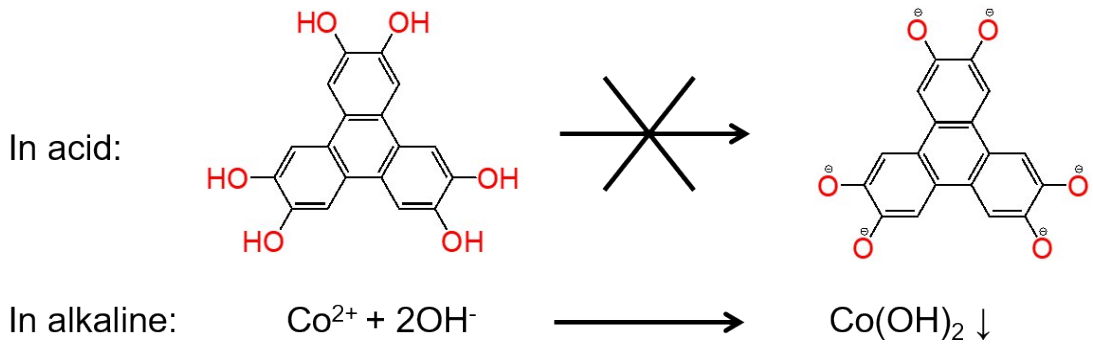

Fig. S14. Reactions happening in acid/alkaline environments in the LB trough of this work.

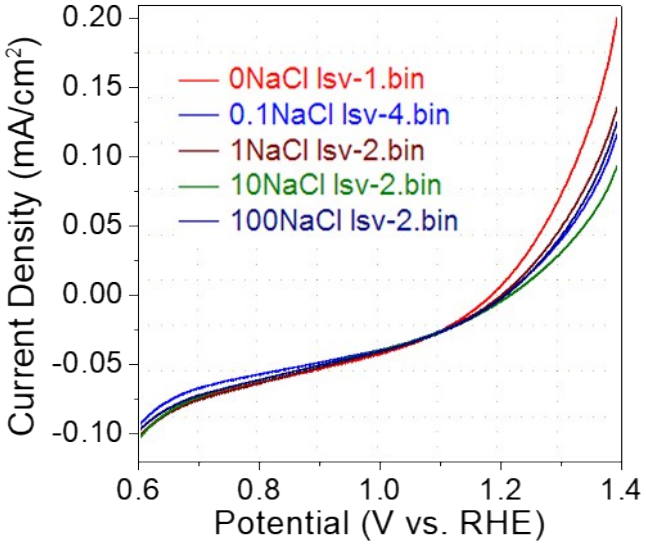

Fig. S15. LSV curves of $[Co_3(HHTP)_2]_n$ LB nanosheets tranferred under different ion concentration.

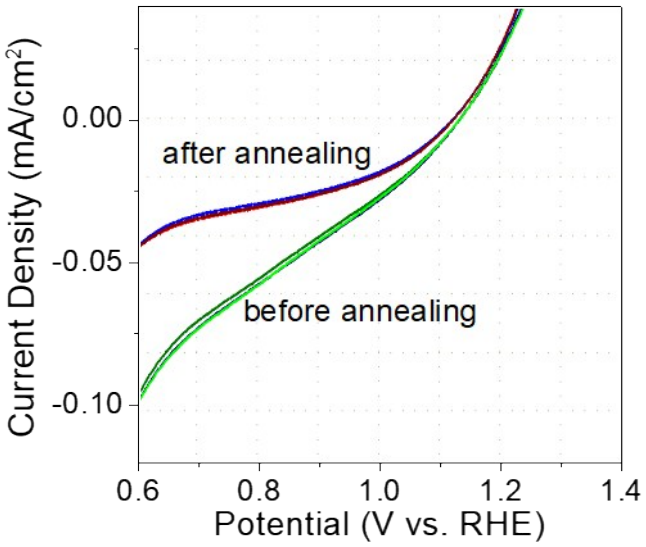

Fig. S16. LSV curves of $[Co_3(HHTP)_2]_n$ LB nanosheets samples before/after 500 ºC annealing for 1h.